Three-Dimensional Structure of the α-Conotoxin GI at 1.2 Å Resolution[†,‡]

L. W. Guddat,[§] J. A. Martin,[§] L. Shan,[∥] A. B. Edmundson,*[,⊥] and W. R. Gray[#]

Centre for Drug Design and Development, University of Queensland, St. Lucia, Queensland 4072, Australia, Harrington Cancer Center, 1500 Wallace Boulevard, Amarillo, Texas 79106, Oklahoma Medical Research Foundation, 825 NE 13th Street, Oklahoma City, Oklahoma 73104, and Department of Biology, University of Utah, Salt Lake City, Utah 84112

Received April 5, 1996; Revised Manuscript Received June 28, 1996[⊗]

ABSTRACT: Predatory marine snails of the genus *Conus* paralyze their fish prey by injecting a potent toxin. The α-conotoxin GI is a 13-residue peptide isolated from venom of *Conus geographus.* It functions by blocking the postsynaptic nicotinic acetylcholine receptor. After crystallization in deionized water, the three-dimensional structure of the GI neurotoxin was determined to 1.2 Å resolution by X-ray crystallography. This structure, which can be described as a trianglar slab, shows overall similarities to those derived by NMR, CD, and predictive methods. The principal framework of the molecule is provided by two disulfide bonds, one linking Cys 2 and Cys 7 and the other Cys 3 and Cys 13. Opposite ends of the sequence are drawn together even further by hydrogen bonds between Glu 1 and Cys 13 and between Cys 2 and Ser 12. Since the C-terminus is amidated, only one negative charge is present (carboxylate of Glu 1), and this is not implicated in receptor binding. Two positively charged regions (the α-amino group of Glu 1 and the guanido group of Arg 9) are situated 15 Å apart at the corners of the triangular face of the molecule. ϕ,ψ angles characteristic of a 3_{10} helix were observed for residues 5−7. For residues 8−11, these angles were consistent with either a type I β-turn or a distorted 3_{10} helix.

Predatory marine snails of the genus *Conus* comprise approximately 500 species with beautiful cone-shaped shells and deadly toxins (Olivera et al., 1985, 1990; Gray et al., 1988). These snails arose in the Eocene period and have adapted to diverse tropical habitats throughout the tropical oceans. They presently constitute one of the most prominent groups of predators inhabiting tropical reefs. Collectively, their prey range over at least five different phyla, including other molluscs, echiuroids, polychaete worms, hemichordates, and fish. Individual *Conus* species, however, tend to focus on a single phylum. Approximately 50 species are piscivorous, immobilizing their victims by venom injected through a disposable, harpoon-like radula tooth (Kohn et al., 1960; Endean & Rudkin, 1963). Larger piscivorous cones such as *Conus geographus* have killed an occasional careless diver, presumably in self defense. In developing venoms effective against such a wide variety of prey, the cones have also provided the scientific community with natural products which have ever expanding potential for medical applications.

More than 200 conotoxins have been isolated from venoms, or their structures have been deduced from studies of cDNA prepared from venom ducts (Woodward et al., 1990). The active agents in these venoms consist mainly of basic peptides 10−30 residues in length and stabilized by two or more intrachain disulfide bonds (Olivera et al., 1985, 1990; Gray et al., 1988). They are thus relatively small compared with the corresponding peptides from snakes, scorpions, and spiders, which more often produce toxins of 40−100 residues (Low & Corfield, 1986; Endo & Tamiya, 1987; Dufton & Hider, 1991; Stiles, 1993; Albrand et al., 1995). Snake toxins tend to fall into the size range of 60−75 residues and act as either neurotoxins or cytotoxins (Endo & Tamiya, 1991; Dufton & Hider, 1991). Many of the conotoxins have detectable activity in the mammalian central nervous system, and some of them share structural similarities with spider toxins (Narasimhan et al., 1994).

Three major classes of paralytic conotoxins have been isolated from piscivorous snails, in addition to vasopressin analogs ("conopressins") and the highly acidic conantokins that target NMDA (*N*-methyl-D-aspartate)-type glutamate receptors. The three classes of paralytic agents, ω, α, and μ, are structurally distinct and attack the neuronal voltage-gated calcium channels, the muscle subtype of nicotinic acetylcholine receptors (AChR), and the voltage-gated sodium channels, respectively (Gray et al., 1981; Olivera et al., 1984; Cruz et al., 1985; Rivier et al., 1987). These targets form successive steps in the activation of muscle contraction by a nerve impulse, so the triple-hit strategy provides for extremely rapid paralysis. The small size and rapid diffusion of the toxins are probably also very important in their biological activity.

Although only minute quantities of the toxins are available from natural sources, their relatively small size permits direct chemical synthesis of multimilligram quantities (Gray et al., 1984). These favorable properties have been pivotal in obtaining enough peptides for the extensive chemical and physiological studies.

The first *Conus* peptide to be isolated and thoroughly characterized was the α-conotoxin GI (from *C. geographus).*

[†] Supported by the Centre for Drug Design and Development, Queensland, Australia, the Harrington Cancer Center, Amarillo, TX, the Oklahoma Medical Research Foundation, Oklahoma City, OK, the Gustavus and Louise Pfeiffer Foundation, and USPHS Grant GM34913.

[‡] The atomic coordinates for this molecule have been deposited in the Brookhaven Protein Data Bank (file name 1NOT).

* To whom correspondence should be addressed.

[§] University of Queensland.

[∥] Harrington Cancer Center.

[⊥] Oklahoma Medical Research Foundation.

[#] University of Utah.

[⊗] Abstract published in *Advance ACS Abstracts,* August 15, 1996.

S0006-2960(96)00820-3 CCC: $12.00

It has the sequence Glu-Cys-Cys-Asn-Pro-Ala-Cys-Gly-Arg-His-Tyr-Ser-Cys-NH_2, with disulfide bonds linking Cys 2−Cys 7 and Cys 3−Cys 13 (Gray et al., 1981). Tight constraints imposed by these disulfide bonds, together with the small size of the peptide, led to reasonable structural models based on modified Chou−Fasman predictive procedures and circular dichroism (CD) measurements (Hider, 1985; Gray et al., 1985). The solution stucture of the GI conotoxin has also been studied by nuclear magnetic resonance (NMR) spectroscopy (Pardi et al., 1989; Kobayashi et al., 1989). The present study was undertaken to provide more accurate stereochemistry of individual amino acids necessary to continue the biochemical and physical chemistry studies and also to provide a basis for modeling other toxins in the series.

In the present study, crystals of GI were obtained from chemically synthesized peptide, and the structure was solved to 1.2 Å resolution by X-ray analysis. A description of this structure will be followed by a comparison with those obtained by alternative techniques.

EXPERIMENTAL PROCEDURES

Peptide Synthesis. The GI peptide was synthesized by solid-phase methods as described previously (Gray et al., 1984). Purification was carried out by reversed-phase HPLC on C18 Vydac columns, using gradients of acetonitrile in either 50 mM triethylamine phosphate (TEAP) at pH 6.0 (Rivier et al., 1987) or 0.1% trifluoroacetic acid (TFA). Before oxidative closure of the disulfide bridges, the linear peptide was purified in the 0.1% TFA system. After oxidation the bicyclic peptide was first fractionated in the TEAP buffer and then rechromatographed in 0.1% TFA. Fractions containing peptide of purity >99%, as judged by isocratic elution with 14% acetonitrile in 0.1% TFA, were pooled and lyophilized.

Crystallization of the GI Peptide. To remove residual TFA, the lyophilized powder was dissolved in 200 μL of 0.05 M NaCl and dialyzed successively against liter quantities of 0.05 M NaCl, 0.01 M NaCl, and deionized water at 4 °C. The peptide solution was then concentrated to 45 mg/mL by placing the dialysis bag in a tray containing dry poly(ethylene glycol) (PEG) 20 000. At 4 °C the peptide spontaneously crystallizes, but the process is much slower at 20 °C. For X-ray diffraction studies, a small crystal from the pool is introduced into a 20 μL droplet of the concentrated peptide solution at room temperature. If the solution is too dilute, the crystal begins to dissolve, and if the solution is too concentrated, the crystal develops branches. Concentration of the droplet by exposure to room air for 10 min is usually adequate to halt the dissolution of the small crystal and dilution of the droplet prevents branching. Between the two extremes, the crystal retains its shape and grows to dimensions of about 1.5 × 0.5 × 0.4 mm in 1 week. For ease of handling, crystals half that size were chosen for X-ray analyses.

The peptide crystallizes in the space group $P2_1$, with a = 14.9 Å, b = 14.6 Å, c = 22.6 Å, and β = 100.2°. These dimensions are compatible with only one toxin molecule in the asymmetric unit and a solvent content of only 27% by volume (Matthews, 1968).

Data Collection and Processing. X-ray diffraction data were first collected to 1.5 Å resolution with an Raxis IIC/RU200 image plate detector system coupled to a Rigaku X-ray generator (University of Queensland). Higher resolution data to 1.1 Å were collected with 2θ set at 44° and a crystal-to-detector distance of 95 mm. Intensities were measured for 24 031 reflections, of which 3597 were unique. The data were 95.8% complete to 1.2 Å, and the overall R_{sym} value was 7.18%. From 1.2 to 1.1 Å, the data were only 54.9% complete, and the R_{sym} value exceeded 30%. However, this high-resolution shell was critical for the initial solution of the crystal structure by direct methods and was therefore included in the data set. Structure factors were converted to normalized E values with the programs BAYES, LEVY, and EVAL (Blessing, 1989). Initial phase angles were calculated with the program SHAKE-AND-BAKE (Miller et al., 1994). One hundred trial structures without geometric constraints were refined with 50 cycles of the SHAKE-AND-BAKE procedure. All 13 residues, with 97 non-hydrogen atoms, were included in the refinements. A histogram of the $R(\psi)$ values showed a bimodal distribution, with 7 of the 100 values in the range of 0.358−0.378. In the Fourier maps based on the seven most probable solutions, the highest four peaks corresponded to the sulfur atoms of the disulfide bonds. The two highest peaks were separated by 2.06 Å and the next highest peaks were 1.97 Å apart, both distances being close to the length (2.04 Å) of a disulfide linkage.

From the solution with the lowest $R(\psi)$ value, coordinates could be assigned to all atoms of four residues (Cys 2, Cys 3, and 7; Gly 8), the backbone atoms (Asn 4, Pro 5, Arg 9, and His 10) and the sulfur atom of Cys 13. These coordinates were used to calculate a $2F_o - F_c$ electron density map at 1.5 Å resolution. After the side chain atoms of Asn 4, Pro 5, Arg 9, and His 10 were identified in this map, the incomplete model was refined by simulated annealing with the program X-PLOR (Brünger et al., 1989). At this stage of the analysis, the R-factor was 0.246 and the R-free value was 0.291 (the latter was calculated with a 10% subset of the X-ray data). The missing atoms were fitted into the electron density of a new $2F_o - F_c$ map, and the structure was then refined to 1.2 Å resolution. To improve the positioning of Glu 1 and Ser 12, we assumed that they might adopt multiple conformations. However, this assumption could not be verified by subsequent difference analyses. Ordered water molecules within hydrogen-bonding distance (<3.2 Å) of nitrogen or oxygen atoms of the peptide (or other water molecules) were identified by examination of $F_o - F_c$ maps and assigned to the crystal structure. After SHELX-93 (Sheldrick, 1993) was used to refine anisotropic temperature (B) factors, the overall R-factor was reduced to 0.149 and the R-free value to 0.178.

Statistics obtained in the final stages of the X-PLOR refinement are presented in Table 1.

RESULTS AND DISCUSSION

General Features of the Three-Dimensional Structure of GI. Three-dimensional "cage" electron density for a 6 Å slice through the molecule is shown in stereo in Figure 1. Density patterns are illustrated in Figure 2 for the three rings in the peptide. A stereo ball-and-stick diagram of the toxin is presented in Figure 3. Figure 4 shows the NMR-derived structures aligned along the α-carbon atoms with the crystallographic structure.

Table 1: Data Collection and Refinement Statistics for GI α-Conotoxin

data collection	
unit cell dimensions (Å)	$a = 14.9$, $b = 14.6$, $c = 22.6$
unit cell angles (deg)	$\alpha = 90$, $\beta = 100.2$, $\gamma = 90$
space group	$P2_1$
no. of observations accepted	24031
no. of observations rejected	689
resolution of data collected $[I > \sigma(I)]$ Å	22.0−1.1
mosaicity	0.313
R-merge (%)	7.18
refinement	
resolution range (Å)	6.0−1.2 Å
no. of unique reflections $[F > 2\sigma(F)]$	2960
completeness of data (%)	95.8
R-factor (isotropic)	0.176
R-free (isotropic)	0.222
R-factor (anisotropic)	0.149
R-free (anisotropic)	0.178
rms deviation in bond length	0.007
rms deviation in bond angles	1.722
rms deviation in dihedral angles	26.77
rms deviation in improper angles	1.41
no. of solvent molecules (H_2O)	21

	ϕ (deg)	ψ (deg)
Glu 1		158.2
Cys 2	−147.0	99.5
Cys 3	−104.5	−4.7
Asn 4	−82.7	147.9
Pro 5	−54.8	−36.0
Ala 6	−63.1	−13.5
Cys 7	−60.9	−30.6
Gly 8	54.3	−124.4
Arg 9	−63.5	−14.2
His 10	−94.5	2.6
Tyr 11	−55.8	128.8
Ser 12	−159.2	104.2
Cys 13	−140.7	

The GI molecule folds in two loops which are closed by the 2−7 and 3−13 disulfide bonds. Only the N-terminal glutamic acid residue lies outside these closed loops, and it can be deleted from the synthesized peptide with no significant loss of biological activity (Almquist et al., 1989). In the mature toxin, the 3−13 disulfide bond ensures that the head and the tail of the peptide will be situated near each other. This portion of the molecule is stabilized further by hydrogen bonds between the γ-carboxyl group of Glu 1 and the α-amido group of Ser 13 (2.8 Å) and between the backbone carbonyl and amide groups (2.8 and 2.9 Å) of Cys 2 and Ser 12, which are oriented in an antiparallel fashion.

It is remarkable that the enzymes responsible for trimming the propeptide to its active form can operate so close to a tightly constrained part of the molecule. These patterns of hydrolysis are found in many other conotoxins. An analogous situation exists with human IgG1 antibodies which are cleaved by papain at the amino end of the threonine residue [no. 225 in Kabat (Kabat et al., 1991)] immediately preceding the first disulfide bond linking the heavy chains in the hinge region (Edmundson et al., unpublished data).

In one view, the peptide assumes the shape of a triangular slab with Glu 1, Arg 9, and Pro 5 at the corners (see Figures 1 and 3). Since the C-terminal Cys 13 is amidated, the only negative charge in the α-conotoxin is the carboxylate side chain of Glu 1. This negative charge is oriented in a direction opposite that of the positively charged side chain of Arg 9.

Both the OE1 and OE2 atoms of Glu 1 are separated from the guanidinium NH2 atom of Arg 9 by 17.9 Å. In a counterclockwise direction along the second edge, the distance between the NH2 atom of Arg 9 and the β-carbon atom of Pro 5 is 16.0 Å. On the third leg of the triangular path, Pro 5 is located 15.0 Å from the carboxyl group of Glu 1. The thickness of the molecule (backbone atoms only) varies between 4.6 and 7.2 Å.

In the Arg 9 and His 10 side chains, the guanido and imidazole groups are oriented outward in the same general direction. They are rotated about 120° away from one another, but their atoms still make a number of van der Waals contacts (3.6 Å). Since the conotoxin was crystallized from deionized water with a measured pH of 5.2, we expected the imidazole group of His 9 (typical pK_a of 6.2) to carry a positive charge. The close proximity of His 10 to the guanido group of Arg 9 can be explained by symmetry contacts in the crystal, chiefly the hydrogen bond between the OD1 atom of Asn 4 with the NE2 group of His 10 (see below).

Tyr 11 lies diametrically opposite the two basic residues. One face of the phenolic ring is flattened against the region occupied by the disulfide bonds (see Figure 3). The phenolic ring alone makes a total of 12 van der Waals contacts with the backbone atoms of Cys 2, Cys 3, Ser 12, and the β-carbon atom of Cys 13. A maximum of 25% of the total surface area of the tyrosine side chain is accessible to a solvent probe of radius 1.4 Å (Connolly, 1983). Although there is no conventional "interior" in this small peptide, Tyr 11 partially seals the disulfide bonds into a hydrophobic "core" region with limited accessibility to solvent in the crystal structure. Unless there is a conformational change resulting in the eversion of tyrosine from such a semiprotected environment, it is unlikely that this side chain is directly involved in the binding of the toxin to its target receptor. This is consistent with the observation that iodination of both His 10 and Tyr 11 does little to diminish biological activity (Gray et al., 1984).

Framework and Hypervariable Loop Residues in the α-Conotoxins. In a loose analogy with immunoglobulins, the disulfide-bridged Cys residues provide the framework for the toxin structure and the others create "hypervariable" loops. The Cys 2−Cys 7 disulfide is a left-handed spiral belonging to a family designated no. 1 by Srinivasan et al. (1990), while the Cys 3−Cys 13 linkage is right-handed and a representative of family no. 5 (independent disulfides). χ values are −91° for the 2−7 S−S and +97° for the 3−13 S−S. The distances between α-carbon atoms are 5.91 Å for Cys 2 and Cys 7 and 5.01 Å for Cys 3 and Cys 13.

Hypervariable regions are found even among members of the same subclass. For example, the MI α-conotoxin retains the same disulfide pattern as GI but has a one-residue extension on the amino end and four substitutions in the other nine hypervariable positions. The N-terminal Glu of GI is replaced by Gly-Arg, while Asn 4 is changed to His, Arg 9 is converted to Lys, and His 10 is altered to Asn (Gray et al., 1981, 1983). These substitutions eliminate one negative charge, add two possible positive charges to the N-terminal segment, and retain the basic properties in position 9. Since the potent antagonists of acetylcholine in receptor binding typically have a preponderance of positive charge, these side

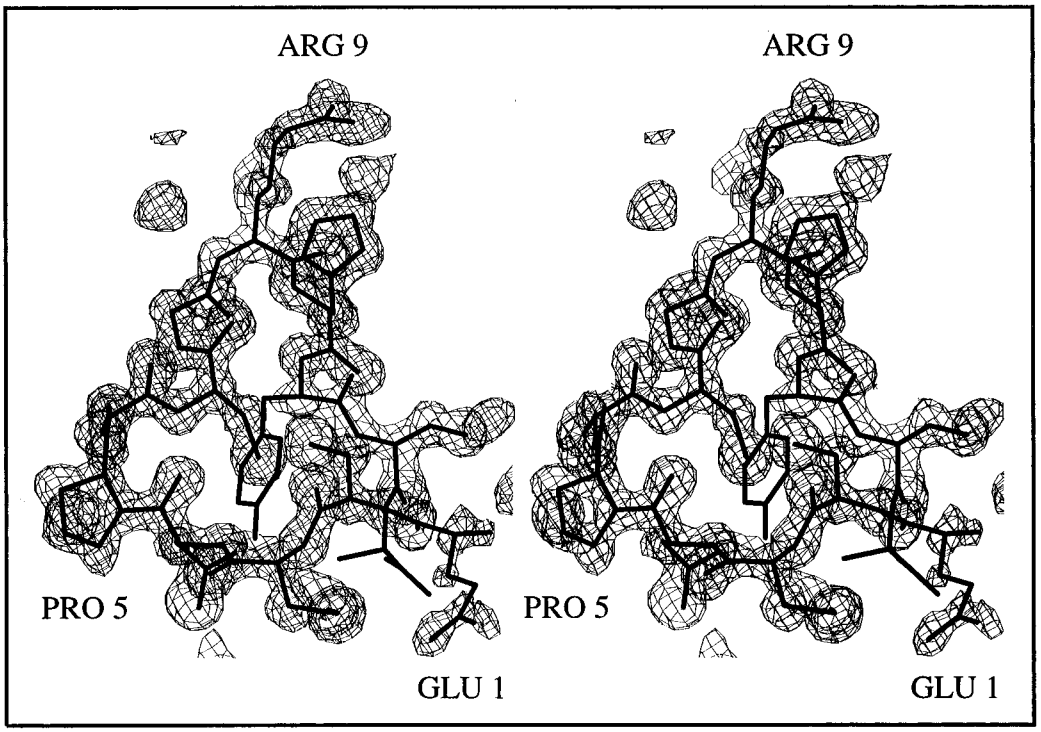

FIGURE 1: $2F_o - F_c$ map at 2σ for the α-conotoxin GI. For clarity, the density shown is for a 6 Å slab, with the GI molecule superimposed.

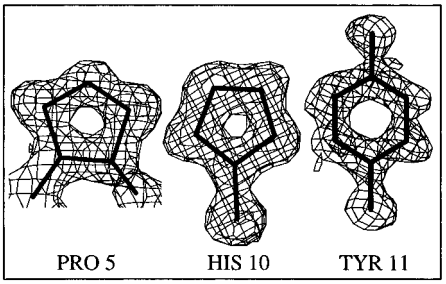

FIGURE 2: $2F_o - F_c$ map at 2σ for the three rings in α-conotoxin GI. The proline ring is puckered, while the other two are planar, aromatic structures. Note the bulges for individual non-hydrogen atoms and the electron-deficient regions in the center of each ring.

chain replacements are consistent with the observed 2.5-fold increase in activity of MI over GI.

As mentioned above, Glu 1 is dispensible for function. In contrast to the bulk of the toxin structure, its side chain methylene groups are not represented by strong electron density (see Figure 1). We have interpreted this observation as evidence for more than one conformation and a paucity of stabilizing interactions with other residues (see Figure 3). Residues occupying positions equivalent to that of Glu 1 are quite variable among even the most closely related "classical" α-conotoxins.

Within this classical series the constituents other than Cys in the loops number either three or five residues. Over a wider range of α-conotoxins, the loops vary markedly in length: e.g., four and three residues in ImI (McIntosh et al., 1994) and four and seven residues in PnI (Fainzilber et al., 1994) and EI (Martinez et al., 1995). These toxins all have the same disulfide patterns but collectively attack different subtypes of acetylcholine receptors.

The only conserved region in the classical series is the tetrapeptide sequence of -Pro-Ala-Cys-Gly- (residues 5−8 in GI). The status of Gly 8 is of special structural interest. In the crystal structure of GI, the measured ϕ, ψ angles (54°, −124°) place residue 8 in the conformational space forbidden to constituents other than glycine. Analog studies have shown that this residue can be substituted by D-Ala in (des-Glu 1)conotoxin GI with only a 30% loss of activity (Almquist et al., 1989). However, substitution of glycine by L-Ala in α-conotoxin MI leads to a 10-fold reduction in potency (Hashimoto et al., 1985). These results suggest that a side chain as small as a methyl group in the L-configuration hinders proper folding of the toxin and/or interferes with the binding to the receptor. Even when in the D-configuration, a large residue preceding Arg 9 is incompatible with the binding requirements. Replacement of Gly 8 by D-Phe in (des-Glu 1) conotoxin GI results in the comprehensive loss of activity (Almquist et al., 1989).

Secondary Structure of the α-Conotoxin GI. The ϕ, ψ angles in the crystal structure of the GI peptide are listed in Table 1. Residues 4−11 are of particular interest for comparisons of the X-ray, NMR, and CD analyses. The NMR results (Pardi et al., 1989) indicated that residues 4−7 and 8−11 form type I β-turns (Wilmot & Thornton, 1988). For these turns, the theoretical ϕ and ψ angles (Richardson, 1981) of the middle two residues are (−60°, −30°) and (−90°, 0°). CD spectra of the GI conotoxin suggested a relatively high content of α- or 3_{10} helices (50%), which could also be localized in this region (Hider, 1985). The ϕ, ψ angles are (−60°, −60°) in α-helices and (−60°, −30°) in 3_{10} helices. While the two types of helix cannot be differentiated by CD, the hydrogen-bonding patterns are definitive: backbone CO to NH hydrogen bonding involves residues i and $i + 4$ in α-helices and residues i and $i + 3$ in 3_{10} helices.

In the X-ray structure, the torsional angles for residues 5−7 and 9−11 cluster around ϕ, ψ angles of −60° and −40° to 0°. These values could generally fit the criteria for β-turns or helices. More importantly, there are four i, $i + 3$ hydrogen bonds in this chain segment: O4−NH7, O5−NH8, O7−

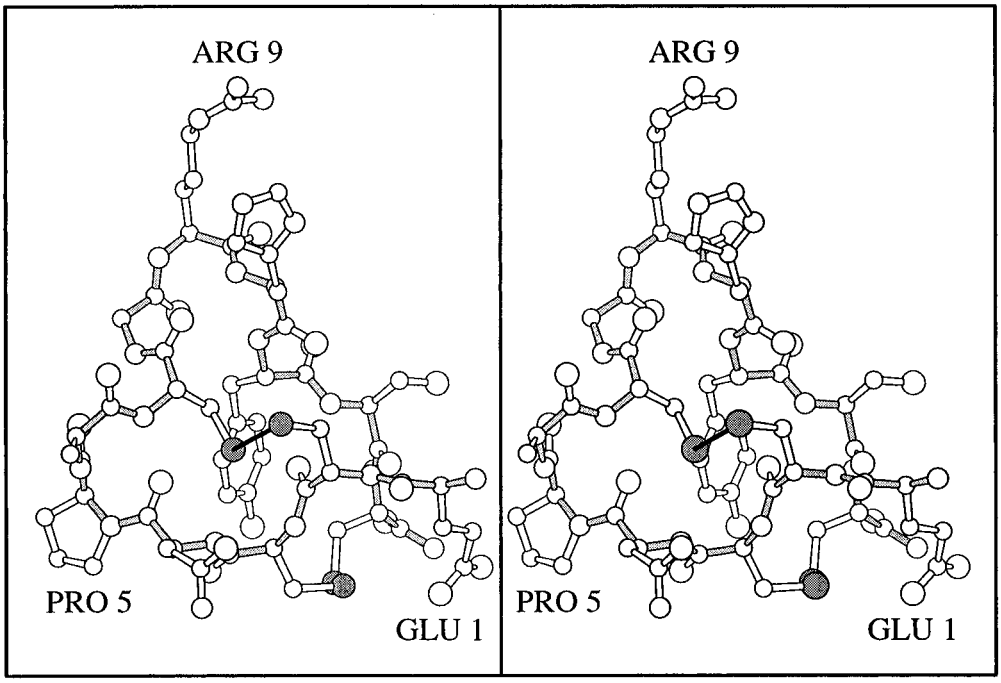

FIGURE 3: Stereo diagram of the non-hydrogen atoms of α-conotoxin GI. The backbone is highlighted in light gray, and the sulfur atoms are in dark gray. Residues 1, 5, and 9 at the corners of the molecule are labeled. The Cys 2−Cys 7 disulfide bond lies above and to the left of the Cys 3−Cys 13 linkage. Note the close proximity of the two ends of the toxin—Glu 1 and Cys 13 behind it at the lower right. The peptide is in the same orientation as in Figure 1.

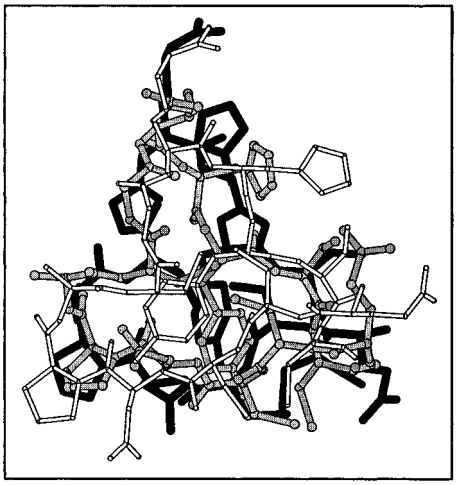

FIGURE 4: Comparison of two of the NMR-derived structures, in gray and white (Pardi et al., 1989), with the crystallographic structure, in black. The structures have been aligned by superimposing their α-carbon atoms.

NH10, and O8−NH11. Oxygen 8 is also within hydrogen-bonding distance of NH10 but is in the incorrect orientation for a linear hydrogen bond. Locally, then the conformation and hydrogen bonding suggest a 3_{10} helix. However, Gly 8 does not have the appropriate ϕ, ψ angles and therefore interrupts the continuity of the helix. Moreover, residues 6 and 9 do not participate in the characteristic i, $i + 3$ hydrogen bonds.

On the other hand, the ϕ, ψ angles for residues 5, 6, 9, and 10 are also appropriate for the central residues of a pair of β-turns. Together, these results suggest two tight turns, best described as a single turn of 3_{10} helix (residues 4−7) followed by a type I β-turn (residues 8−11). The latter segment could also be considered a distorted 3_{10} helix, since these descriptions are not mutually exclusive. Overall, the assignments of secondary structure by X-ray crystallography are compatible with the observations made previously with NMR and CD techniques.

Ordered Water Molecules in the Crystal Structure. Despite the apparently open spaces in the electron density map of the disulfide-linked loops in Figure 3, there are no ordered water molecules in the "internal" parts of the peptide. Within 4 Å of atoms on the external surfaces of the peptide, 21 ordered solvent molecules have been identified. Four of these are located within hydrogen-bonding distances of the guanido nitrogens of Arg 9, three are associated with the hydroxyl group of Ser 12, and two are situated near the side chain amide group of Asn 4. The Glu 1 carboxyl group and the Tyr 11 hydroxyl group interact with only one water molecule each. Ten solvent molecules form hydrogen bonds with backbone carbonyl and amide groups.

Packing of Peptide Molecules in the Crystal Lattice. Among the 35 contacts among symmetry-related molecules, only three involve hydrogen bonds: (1) the carboxylate group (atom OE1) of Glu 1 with the phenolic group (OH) of Tyr 11 in an adjacent molecule, (2) the backbone carbonyl oxygen of Cys 3 with the terminal amide group (ND2) of Cys 13, and (3) the OD1 atom of Asn 4 with the imidazolium group (NE2) of His 10. Hydrogen bond no. 1 may be one of the interactions critical for promoting crystallization of the toxin. In addition to hydrogen bond no. 2, only seven other backbone atoms (from Pro 5, Gly 8, and Arg 9) make contacts with neighboring molecules. Collectively, these interactions are too weak to exert significant effects on the backbone conformation in the crystal structure. However, the outer parts of the Arg 9 side chain are pressed against Tyr 11 of a symmetry-related molecule. No counterions are detectable at the tip of Arg 9, and it seems likely that the packing interactions dictate the resting place of the Arg side chain in the crystal.

Interactions with the Acetylcholine Receptor. At the neuromuscular junction, acetylcholine acts by binding to the

nicotinic AChR. This is a ligand-activated sodium channel protein, consisting of five homologous subunits (α_2, β, γ, δ) arranged as a rosette around a central axis, which also defines the course of the sodium channel (Unwin, 1993, 1995). The channel is transiently converted from a closed to an open state by the binding of two molecules of acetylcholine to sites located at the $\alpha-\gamma$ and $\alpha-\delta$ interfaces. Several lines of evidence indicate that these sites are distant from each other and probably located on the outside of the rosette (Johnson et al., 1987; Unwin, 1993, 1995).

Conotoxin GI and many other antagonists compete with acetylcholine for these sites. Binding of a single antagonist molecule is sufficient to prevent opening of the channel. Antagonists probably act by preventing a conformational change rather than by blocking the channel.

Their affinities vary widely among species, with receptor subtypes, and even between the two sites on a single receptor molecule. At the murine muscle nicotinic AChR, conotoxin GI binds about 45 000 times more tightly to the $\alpha-\delta$ than to the $\alpha-\gamma$ site. Conotoxin MI generally follows the same pattern as GI (Kreienkamp et al., 1994), but SI is 100-fold less selective (Groebe et al., 1995). In *Torpedo* AChR, the GI peptide exhibits the opposite site selectivity, and SI does not discriminate between the two sites (Hann et al., 1994).

Recently, it has been shown that the critical difference between GI and SI lies in position 9 (Gray et al., 1995). Replacement of Pro 9 in the sequence of SI by lysine dramatically restores the high affinity and selectivity associated with GI (Gray et al., 1995). Although an appropriately placed positive charge has long been thought to be a critical component of AChR antagonists, the substitution of a neutral residue (e.g., alanine or norleucine) for Arg 9 in GI or the homologous Lys 10 in MI leads to only a modest alteration in activity (Gray et al., 1985; Hashimoto et al., 1985). It is therefore possible that a significant change in the conformation of the second disulfide loop in the modified SI molecule is largely responsible for the observed functional effects of the Pro-Lys interchange. The imminent completion of high-quality NMR analyses of conotoxin SI and several analogs will allow us to distinguish between the alternative explanations (D. J. Christensen, W. R. Gray, R. A. Myers, B. M. Olivera, and C. D. Poulter, unpublished results).

In parallel with the studies on natural and synthetic variants of the α-conotoxins, mutational analyses are beginning to pinpoint residues within the nicotinic AChR that confer specificity to the interactions with the toxins (Sine et al., 1995). These complementary approaches should provide a wealth of new insight into the overall architecture and reactivity of these receptors with the small but lethal conopeptides.

The α-neurotoxins from elapid venoms also interact with the nicotinic AChR and interfere with its binding to acetylcholine. For classification, they can be divided into two groups, the short chain molecules of 60−62 residues and the long chain toxins of 70−74 residues. Examples of short chain molecules examined by X-ray and NMR techniques are the erabutoxins from sea snake venoms (Tsernoglou & Petsko, 1976; Low & Corfield, 1986; Saludjian et al., 1992; Hatanka et al., 1994). Long chain molecules subjected to X-ray analyses include a cobratoxin (Walkinshaw et al., 1980) and a krait bungarotoxin (Agard & Stroud, 1982). In all of these structures there is a relatively rigid core stabilized by four disulfide bonds. Three finger-like loops emanating from the core are implicated in the binding to the AChR. By mutagenic experiments, for example, the following components at the tip of the central loop in erabutoxin *b*, Lys 27, Trp 29, Asp 31, Phe 32, and Arg 33, have been identified as important residues for AChR binding (Pillet et al., 1993). Some of these side chains are not well defined in the NMR structure, an indication of probable mobility in solution (Hatanka et al., 1994).

From these studies, it is generally agreed that the disulfide-rich core in snake α-neurotoxins provides a relatively stable base for the flexible loops to make multipoint attachments to the target receptor. Though miniaturized, the disulfide scaffolding and hypervariable stretches of other residues recapitulate the theme in the α-conotoxin chains.

Biological Implications. Ligand-gated ion channels are the focus of intense interest because of their central role in brain function. Multiple isoforms for each channel protein occur, with specialized functions and often highly localized distributions in particular nerve tracts. The muscle subtype of the acetylcholine receptor is closely homologous with a large family of subtypes from brain, yet the various α-conotoxins show exquisite discrimination among them. Understanding the structural basis of this selectivity is a key step toward rational design of precisely acting neuropharmacological agents. A dramatic example of this approach is the clinical testing of ω-conotoxin MVIIA as a highly selective blocker of a subset of spinal cord neurons responsible for the transmission of pain signals (Gibbs, 1996). Infusion of the toxin appears to relieve intractable pain in patients who have become tolerant to the effects of massive doses of opiates.

The α-conotoxin described in this paper is smaller than the MVIIA ω-type molecule. Thirteen amino acid residues are locked into a relatively compact and well-defined shape by two disulfide bonds, one anchoring a six-membered loop between residues 2 and 7 and the second irreversibly securing the tail at residue 13 to residue 3. Only one residue, Glu 1, lies outside the the disulfide-linked loops, and it is not essential for activity. Thus the MI toxin has been enzymatically trimmed in the snail to practically the theoretical limit compatible with a cyclic structure and the paralytic power of the $\omega-\alpha-\mu$ triad of molecules to halt muscle contraction abruptly in the prey.

The present study provides a high-resolution structure that will serve as a benchmark for comparison with NMR-derived structures of similar molecules, in solution and bound to the receptor.

ACKNOWLEDGMENT

We thank Dr. Arthur Pardi, University of Colorado, for providing atomic ccordinates of the NMR-derived molecules of GI. We also thank Kim Andersen for her help in preparing the figures and manuscript for publication.

REFERENCES

Agard, D. A., & Stroud, R. M. (1982) *Acta Crystallogr., Sect. A 38*, 186−194.

Albrand, J.-P., Blackledge, M. J., Pascaud, F., Hollecker, M., & Marion, D. (1995) *Biochemistry 34*, 5923−5937.

Almquist, R. G., Kadambi, S. R., Yasuda, D. M., Weitl, F. L., Polgar, W. E., & Toll, L. R. (1989) *Int. J. Pept. Protein Res. 34*, 455−462.

Blessing, R. H. (1989) *J. Appl. Crystallogr. 22*, 396−397.
Brünger, A. T., Karplus, M., & Petsko, G. A. (1989) *Acta Crystallogr. A45*, 50−61.
Connolly, M. L. (1983) *Science 221*, 709−713.
Cruz, L. J., Gray, W. R., Olivera, B. M., Zeikus, R. D., Kerr, L., Yoshikami, D., & Moczydlowski, E. (1985) *J. Biol. Chem. 260*, 9280−9288.
Dufton, M. J., & Hider, R. C. (1991) in *Snake Toxins* (Harvey, A. L., Ed.) pp 259−302, Pergamon Press, New York.
Endean, R., & Rudkin, C. (1963) *Toxicon 1*, 49−64.
Endo, T., & Tamiya, N. (1987) *Pharmacol. Ther. 34*, 403−451.
Endo, T., & Tamiya, N. (1991) in *Snake Toxins* (Harvey, A. L., Ed.) pp 165−222, Pergamon Press, New York.
Fainzilber, M., Hasson, A., Oren, R., Burlingame, A. L., Gordon, D., Spira, M. E., & Zlotkin, E. (1994) *Biochemistry 33*, 9523−9529.
Gibbs, W. W. (1996) *Sci. Am. 274* (2), 28−29.
Gray, W. R., Luque, A., Olivera, B. M., Barrett, J., & Cruz, L. J. (1981) *J. Biol. Chem. 256*, 4734−4740.
Gray, W. R., Rivier, J. E., Galyean, R., Cruz, L. J., & Olivera, B. M. (1983) *J. Biol. Chem. 258*, 12247−12251.
Gray, W. R., Luque, F. A., Galyean, R., Atherton, E., Sheppard, R. C., Stone, B. L., Reyes, A., Alford, J., McIntosh, M., Olivera, B. M., Cruz, L. A., & Rivier, J. (1984) *Biochemistry 23*, 2796−2802.
Gray, W. R., Middlemas, D. M., Zeikus, R., Olivera, B. M., & Cruz, L. J. (1985) in *Peptides: Chemistry and Biology (9th American Peptide Symposium)* (Deber, C. M., Hruby, V. J., & Kopple, K. D., Eds.) pp 823−832, Pierce Chemical, Toronto.
Gray, W. R., Olivera, B. M., & Cruz, L. J. (1988) *Annu. Rev. Biochem. 57*, 665−700.
Gray, W. R., Palmieri, S. J., Christensen, D. J., Groebe, D. R., & Abramson, S. N. (1995) *Soc. Neurosci. Abstr. 21*, 10.
Groebe, D. R., Dumm, J. M., Levitan, E. S., & Abramson, S. N. (1995) *Mol. Pharmacol. 48*, 105−111.
Hann, R. M., Pagán, O. R., & Eterovic, V. A. (1994) *Biochemistry 33*, 14058−14063.
Hashimoto, K., Uchida, S., Yoshida, H., Nishiuchi, Y., Sakakibara, S., & Yukari, K. (1985) *Eur. J. Pharmacol. 118*, 351−354.
Hatanka, H., Miyuki, O., Khoda, D., Tate, S.-i., Suda, A., Tamiya, N., & Inagaki, F. (1994) *J. Mol. Biol. 240*, 155−166.
Hider, R. C. (1985) *FEBS Lett. 184*, 181−184.
Johnson, D. A., Brown, R. D., Herz, J. M., Berman, H. A., Andreasen, G. L., & Taylor, P. (1987) *J. Biol. Chem. 262*, 14022−14029.
Kabat, E. A., Wu, T. T., Perry, H. M., Gottesman, K. S., & Foeller, C. (1991) *Sequences of Proteins of Immunological Interest*, 5th ed., Public Health Service, U.S. Department of Health and Human Services, National Institutes of Health, Bethesda, MD.
Kobayashi, Y., Ohkubo, T., Kyogoku, Y., Nishiuchi, Y., Sakakibara, S., Braun, W., & Go, N. (1989) *Biochemistry 28*, 4853−4860.
Kohn, A. J., Saunders, P. R., & Wiener, S. (1960) *Ann. N.Y. Acad. Sci. 90*, 706−725.
Kreienkamp, H.-J., Sine, S. M., Maeda, R. K., & Taylor, P. (1994) *J. Biol. Chem. 269*, 8108−8114.
Low, B. W., & Corfield, P. W. R. (1986) *Eur. J. Biochem. 161*, 579−587.
Martinez, J. S., Olivera, B. M., Gray, W. R., Craig, A. G., Groebe, D. R., Abramson, S. N., & McIntosh, J. M. (1995) *Biochemistry 34*, 14519−14526.
Matthews, B. W. (1968) *J. Mol. Biol. 33*, 491−497.
McIntosh, J. M., Yoshikami, D., Mahe, E., Nielsen, D. B., Rivier, J. E., Gray, W. R., & Olivera, B. M. (1994) *J. Biol. Chem. 269*, 16733−16739.
Miller, R., Gallo, S. M., Kahlak, H., & Weeks, C. M. (1994) *J. Appl. Crystallogr. 27*, 613−621.
Narasimhan, L., Singh, J., Humblet, C., Guruprasad, K., & Blundell, T. (1994) *Struct. Biol. 1*, 37−45.
Olivera, B. M., McIntosh, J. M., Cruz, L. J., Luque, F. A., & Gray, W. R. (1984) *Biochemistry 23*, 5087−5095.
Olivera, B. M., Gray, W. R., Zeikus, R., McIntosh, J. M., Varga, J., Rivier, J., de Santos, V., & Cruz, L. J. (1985) *Science 230*, 1338−1343.
Olivera, B. M., Rivier, J., Clark, C., Ramilo, C. A., Corpuz, G. P., Abogadie, F. C., Mena, E. E., Woodward, S. R., Hillyard, D. R., & Cruz, L. J. (1990) *Science 249*, 257−263.
Pardi, A., Galdes, A., Florance, J., & Maniconte, D. (1989) *Biochemistry 28*, 5494−5501.
Pillet, L., Tremeau, F., Ducancel, F., Drevet, P., Zinn-Justin, S., Pinkasfeld, S., Boulain, J. C., & Ménez, A. (1993) *J. Biol. Chem. 268*, 909−916.
Richardson, J. S. (1981) *Adv. Protein Chem. 34*, 167−339.
Rivier, J., Galyean, R., Simon, L., Cruz, L. J., Olivera, B. M., & Gray, W. R. (1987) *Biochemistry 26*, 8508−8512.
Saludjian, P., Prange, T., Navaza, J., Ménez, R., Guilloteau, J. P., Ries-Kautt, M., & Ducruix, A. (1992) *Acta Crystallogr., Sect. B 48*, 520−531.
Sheldrick, G. M. (1993) Ph.D. Thesis, University of Göttingen, Göttingen, Germany.
Sine, S. M., Kreienkamp, H.-J., Bren, N., Maeda, R., & Taylor, P. (1995) *Neuron* (in press).
Srinivasan, N., Sowdhamini, R., Ramakrishnan, C., & Balaram, P. (1990) *Int. J. Pept. Protein Res. 36*, 147−155.
Stiles, B. G. (1993) *Toxicon 31*, 825−834.
Tsernoglou, D., & Petsko, G. A. (1976) *FEBS Lett. 68*, 1−4.
Unwin, N. (1993) *J. Mol. Biol. 229*, 1101−1124.
Unwin, N. (1995) *Nature 373*, 37−43.
Walkinshaw, M. D., Saenger, W., & Maelicke, A. (1980) *Proc. Natl. Acad. Sci. U.S.A. 77*, 2400−2404.
Wilmot, C. M., & Thornton, J. M. (1988) *J. Mol. Biol. 203*, 221−232.
Woodward, S. R., Cruz, L. J., Olivera, B. M., & Hillyard, D. R. (1990) *EMBO J. 9*, 1015−1020.

BI960820H